Substrate-Dependent Properties of Polydiacetylene Nanowires on Graphite and MoS_2

Rajiv Giridharagopal and Kevin F. Kelly*

Department of Electrical and Computer Engineering and Rice Quantum Institute, Rice University, Houston, Texas 77005

ARTICLE

ABSTRACT Scanning tunneling microscopy (STM) has been used to study polydiacetylene (PDA) nanowires and their electronic coupling with the surface. PDA nanowires exhibit intriguing substrate-dependent electronic effects when probed at varying sample bias voltage conditions on different substrate electrode materials, in this case, highly ordered pyrolytic graphite (HOPG) and molybdenum disulfide (MoS_2). An analysis of nanowire heights over a wide range of bias voltages shows strong polymer—substrate contact effects, the strength of which is reflected in the asymmetry of the height—voltage data on each substrate. On HOPG, PDA nanowires exhibit a decrease in height as the bias voltage magnitude is reduced, and the height is substantially greater at negative voltages than at positive voltages. On MoS_2, PDA nanowires appear with much higher contrast than on HOPG when imaged at the same negative bias conditions. At positive bias voltages on MoS_2, the nanowires are invisible in all STM images, yet the unpolymerized molecules can still be imaged. These effects are necessarily electronic in origin. Surprisingly, only the polymer nanowires exhibit any bias-dependent change; the unpolymerized molecules are imaged at all bias voltages on both substrates. Additionally, the substrate affects how the unpolymerized molecules are ordered. In some areas, the molecules are arranged such that part of the monolayer is offset from the correct threefold symmetry direction by a slight misfit angle. On HOPG, this misfit is approximately 6°, while on MoS_2, it is approximately 11°. Interactions with the substrate thus play a role both in electronic structure and in molecular alignment.

KEYWORDS: polydiacetylene · organic nanowires · scanning tunneling microscopy · molybdenum disulfide · graphite

One of the barriers to the further development of organic and molecular electronics is the currently incomplete understanding of charge transfer at the polymer—electrode interface. For example, the choice of electrode materials is known to play a key role in the contact resistance in organic field effect transistors.[1,2] Interfacial properties are increasingly important in the realm of molecular electronics.[3,4] A related issue with molecular electronics is that of interconnects, namely, the lack of a controllable, high conductivity organic wire to connect various switching elements. One such candidate nanowire material is polydiacetylene. Polydiacetylene (PDA) is a semiconducting polymer of the form $(=C-C\equiv C-C=)_n$ that exhibits increased conductivity when doped with iodine.[5–7] As a molecular interconnect, PDA nanowires offer an advantage over other organic nanostructures in that they can be controllably formed on the surface of an ordered monolayer of diacetylene derivative molecules. The molecules can be polymerized to form PDA nanowires by applying a voltage pulse at certain locations with the scanning tunneling microscopy tip, as was first shown by Okawa and Aono.[8,9] PDA nanowires have been studied using scanning tunneling microscopy (STM) at solid—air,[8–10] solid—liquid,[11–13] and solid—vacuum interfaces.[14] In addition, thin films of PDA have been used in technological applications such as monolayer organic field effect transistors[15–17] and photovoltaic devices.[18] While the electronic behavior of PDA nanowires on graphite has been studied previously,[19,20] atomic-scale investigations have not addressed the significant issue of substrate-dependent PDA nanowire behavior.

We report here our recent work using scanning tunneling microscopy and spectroscopy to analyze PDA nanowires across a range of sample bias voltages and on two different substrate materials, highly ordered pyrolytic graphite (HOPG) and molybdenum disulfide (MoS_2). MoS_2, a semiconducting transition metal dichalcogenide, has a layered structure similar to that of HOPG.[21] Images of bare MoS_2 exhibit large, flat terraces like those on HOPG, but MoS_2 surfaces have a higher number of surface defects. MoS_2 has a lattice constant of 0.316[22] *versus* 0.246 nm[23] for HOPG. In addition, MoS_2 has a greater work function (anywhere from 4.6[24] to 4.9 eV[25] depending on the report) than HOPG (4.48[26] to 4.6 eV[27]). Also, the fact that MoS_2 is a semiconductor with a band gap reported between 1.2[25]

*Address correspondence to kkelly@rice.edu.

Received for review May 13, 2008 and accepted June 20, 2008.

Published online July 26, 2008.
10.1021/nn800287x CCC: $40.75

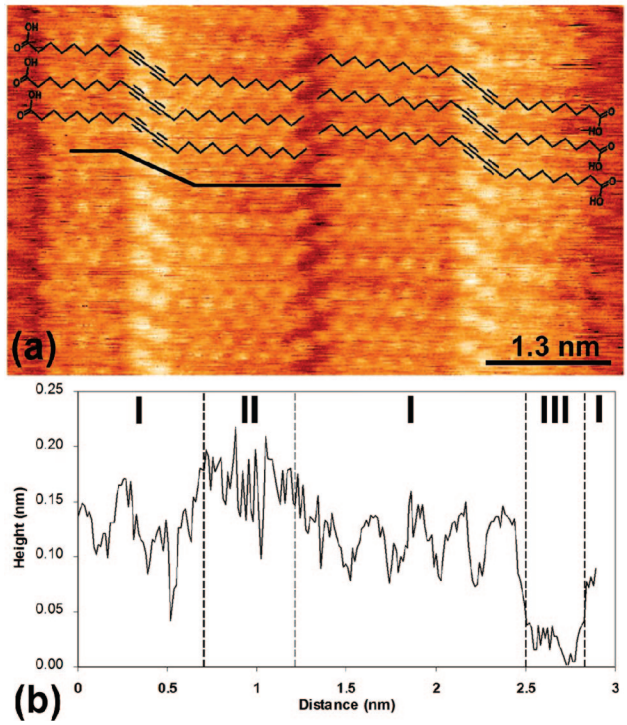

Figure 1. (a) Atomic resolution image of two ordered, unpolymerized PCDA stripes on a HOPG surface (6.5 nm × 3.9 nm, −1.3 V, 3.5 pA). The schematic overlay shows how the molecules are ordered on the surface. The bright points in the center of each column are the diacetylene moieties, with the two triple-bonded regions appearing as bright protrusions. (b) Height cross section along the path indicated by the black line in image (a), divided to indicate the different regions of the PCDA molecule: the alkyl chains (I), the diacetylene moiety (II), and the graphite substrate imaged in the gap between columns of molecules (III).

and 1.4 eV[24] makes it an interesting substrate electrode material that may further elucidate various transport properties of polydiacetylene. The two different substrates thus provide a rich set of contrasting properties for investigating material-dependent effects in PDA wires. Because of the nature of STM, the height of the nanowire structures can be used to explore such effects.

RESULTS AND DISCUSSION

The atomic resolution capability of STM allows for unique information to be gleaned from a surface aside from just topography. This is because STM images are necessarily a convolution of electronic and topographic structure due to the nature of electron tunneling.[28] As a result, features which appear taller in an STM image may in fact appear so because of electronic effects. Such is the case in Figure 1, where two parallel columns of unpolymerized 10,12-pentacosadiynoic acid (PCDA) molecules are shown with atomic resolution. PCDA is a diacetylene derivative molecule that can be subsequently polymerized to form PDA nanowires. The PCDA ordering is shown schematically, for clarity. The bright bumps in the center of each column are the diacetylene moieties in each PCDA molecule. The height cross section indicates that the typical height of a diacetylene moiety is approximately 0.12−0.17 nm. Although there are four carbon molecules in diacetylene, the STM images the two carbons in each triple bond indistinguishably, presumably due to the delocalization of the electrons within the π orbitals. The diacetylene moiety in each PCDA molecule is brighter than the neighboring alkyl chains because of the enhanced electronic charge transfer in multiple carbon bond structures.[29] While the STM image implies that the diacetylene groups are topographically higher on the surface, they are actually in the plane with the alkyl chains in each molecule.[9,10,30]

Before discussing the difference in nanowire images on the two substrates, it is instructive to look at how the substrate influences the molecular ordering of PCDA. The PCDA molecules self-order on the HOPG and MoS_2 substrates and exhibit threefold symmetry commensurate to that of the underlying material.[9−11] This is probably due to an epitaxial arrangement of the alkyl side chains on the surface, similar to that observed for various other materials on both substrates.[31,32] However, PCDA does not seem to self-assemble on other surfaces of interest such as Au(111). While typically the monolayers exhibit domains wherein the molecules are only oriented in three possible directions, Figure 2a,b (on HOPG and MoS_2, respectively) shows that the monolayers can sometimes exhibit a slight misfit angle from the preferred orientation. The colored arrows in these images emphasize the observed misfit angles. To better clarify this effect, Figure 2c,d shows the 2D fast Fourier transform (FFT) images of the two STM images. In Figure 2c, two of the three symmetry directions exhibit such an effect. The misfit angle of PCDA on HOPG is approximately 6°, in agreement with the misfit found for poly(3-hexylthiophene) on HOPG,[33] while on MoS_2, the misfit angle is approximately 11°. Observations of such misfit angles were not common, but among the samples with misfits, the angles varied from 5 to 7° on HOPG and 11 to 13° on MoS_2. The difference in misfit angles may be partially due to the different lattice constants, given that molecular ordering is influenced by both the lattice constant and interactions with the substrate.[34]

Regardless of the ordering differences, nanowires can be formed on both substrates by irradiating the unpolymerized PCDA molecules with ultraviolet light, producing nanowires of different lengths on the surface. Typical STM images of PDA nanowires on HOPG and MoS_2 are shown in Figure 3, with both images mapped to the same color scale. The unpolymerized PCDA molecules from Figure 1 appear as alternating stripes in the background, while the PDA nanowires appear as bright features on the surface with a much higher contrast than the surrounding film. The PCDA monolayer appears the same on both substrates, though the monolayer on MoS_2 exhibits a number of regular MoS_2 sur-

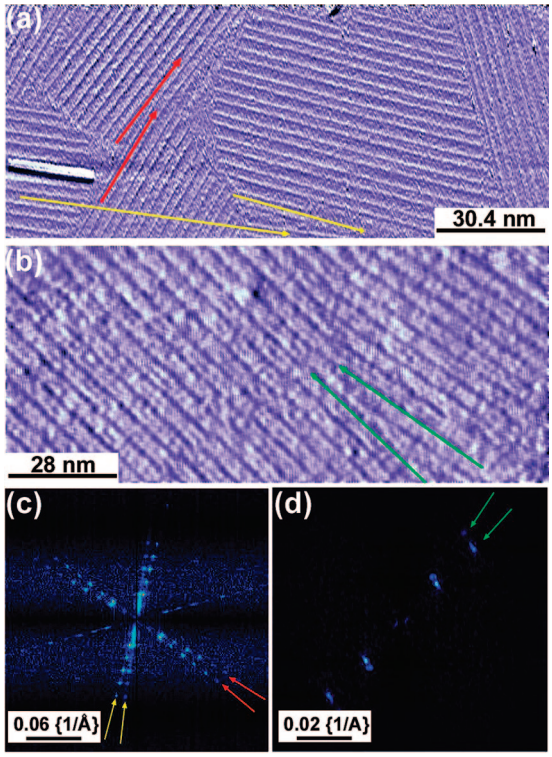

Figure 2. Examples of typical PCDA monolayers exhibiting misfit angles on (a) HOPG and (b) MoS_2. The PCDA monolayer on HOPG shows all three expected orientations, but two different misfits, as well. The monolayer shown on MoS_2 only exhibits one direction and thus only a single misfit. The misfit directions are clarified by the red and yellow lines on HOPG and the green lines on MoS_2. The 2D FFT images are shown in (c) and (d). In (c), all three directions are observed, and the misfit angles are also visible as expected from the red and yellow lines corresponding to the same features in (a). The misfit angle between each set of lines is approximately 6°. In (d), the misfit angle on the MoS_2 is also evident. In this case, the misfit angle is approximately 11°. Imaging conditions: (a) −1.0 V, 10 pA, 152 × 65 nm^2; (b) +1.3 V, 5 pA, 140 × 61 nm^2. Images (a) and (b) were derivative-filtered to improve clarity.

face defects not seen on HOPG. The MoS_2 surface defects appear brighter than the PCDA monolayer on the surface. The defects are measured to be approximately 0.5 nm high relative to the PCDA monolayer, which is more than that of the diacetylene moiety in the PCDA monolayer on the surface. Interestingly, on MoS_2, the nanowires are substantially brighter than on HOPG despite the nanowires having been formed and prepared the same way on both substrates. Because the nanowires are the same material on both substrates, the difference in heights must be due to electronic effects.

The nanowires in the STM images appear as bright structures relative to the PCDA background because of both electronic effects and the lifted-up conformation of the PDA nanowire upon polymerization. The lifted-up conformation was previously proposed based on STM data.[9,10] More recently, Okawa *et al.* used atomic force microscopy (AFM) on similarly prepared samples on HOPG and determined the height of the

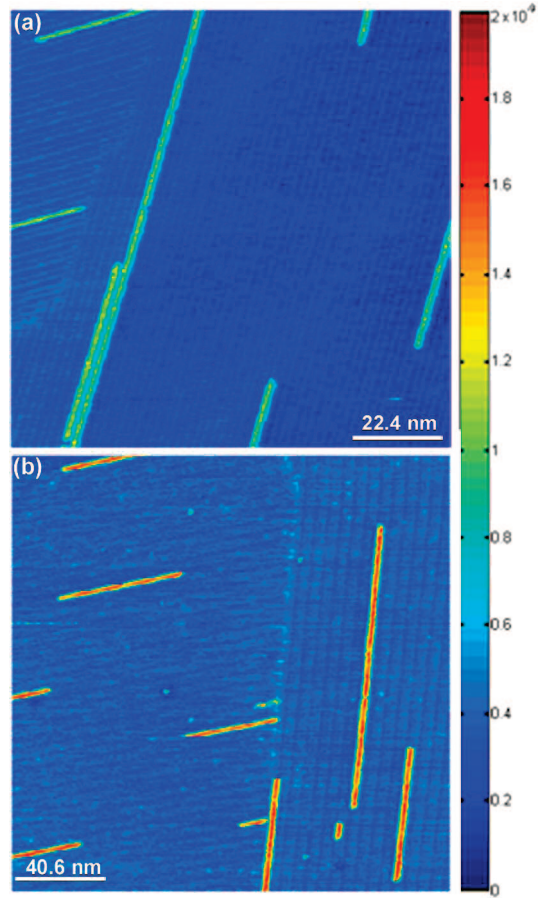

Figure 3. Typical images of PDA wires on (a) HOPG and (b) MoS_2, with the same color scale. The false coloring in the image reflects a measured height range of 2 nm. Imaging conditions: (a) −1.0 V, 10 pA, 112 × 112 nm^2; (b) −1.23 V, 5 pA, 203 × 203 nm^2.

nanowires to be approximately 0.13 nm. They also performed density functional calculations for comparison, which yielded a height of 0.146 nm.[35] This height is the result of the subsequent conformational change after polymerization. The heights reported here by STM are substantially greater, which is to be expected given the increased conductivity of the PDA backbone and the influence of electronic structure on height in STM images. For example, the nanowires on HOPG in Figure 3 are approximately 0.7 nm high, a difference of nearly 0.55 nm from the AFM data. The remainder of this paper focuses on electronic contributions to the height, particularly those specific to the substrate.

Another set of PDA nanowires on HOPG and MoS_2 are shown in Figure 4 along with their height profiles. The boxed regions indicate where height profile averaging was performed. The height profiles along the axis perpendicular to the nanowires in the boxed area were averaged together, resulting in the height profiles shown (see the Methods section for more information). Figure 4 shows that the PDA heights differ substantially between the two substrates. The nanowire in the MoS_2 image is measured to be 1.02 nm tall, whereas the three nanowires in the HOPG image measure 0.71,

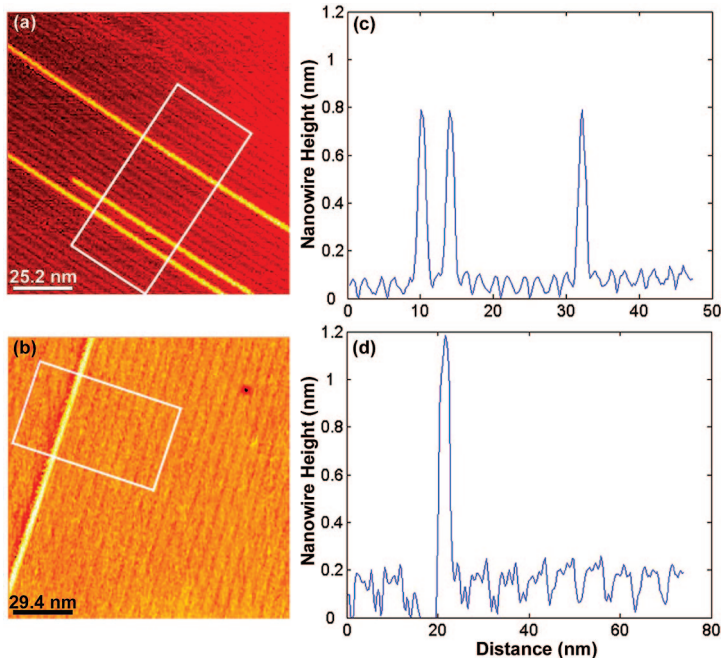

Figure 4. Images of PDA nanowires on (a) HOPG and (b) MoS_2, along with averaged height cross sections in (c) and (d), respectively. The white boxes in the STM images indicate the region where the height profiles (taken along the direction perpendicular to each nanowire) were averaged together to produce the resulting cross-sectional data. (c) The nanowire heights on HOPG are 0.71, 0.71, and 0.72 nm from left to right. (d) The nanowire height on MoS_2 is 1.05 nm. Imaging conditions: (a) −1.0 V, 10 pA, 126 × 126 nm^2 and (b) −1.0 V, 5 pA, 147 × 147 nm^2.

0.71, and 0.72 nm tall. The heights are measured as the difference between the average peak nanowire height in the box and the average height of the surrounding PCDA monolayer. Similar height values were found on many other HOPG and MoS_2 samples, with an overall average PDA height of 0.65 nm on HOPG and 1.00 nm on MoS_2 at −1.0 V.

To further evaluate the electronic effects on STM-measured heights, we changed the applied voltage polarity during imaging. When imaging conditions are set to negative and positive sample bias voltages, STM images reflect occupied and unoccupied electron states, respectively. In other words, the system images hole carriers at negative sample bias voltages and electron carriers at positive voltages. Thus, for the same system, it is possible to see striking differences depending on the voltage polarity that can also provide spectroscopic information.[36] This is shown in Figure 5 for nanowires on HOPG. The images in Figure 5 were simultaneously acquired at −1.0 and +1.0 V. Each individual line was scanned first at one voltage, then the bias was changed and the same line was acquired at the second voltage; the voltage alternates in this way through all 512 lines in the image. This technique, sometimes called "multi-volt imaging," allows for direct comparison of different imaging conditions by negating thermal drift and other perturbations such as nanowire desorption[13,14] that can occur with sequential imaging.

The PDA nanowire in the positive bias voltage image exhibits much lower contrast than in the negative bias voltage image. PDA nanowires appear with different heights depending on the state being probed, similar to the effect observed for napthalocyanine deposited on HOPG.[37] The PCDA monolayers do not exhibit any significant change in height based on the bias voltage magnitude or polarity. The gap between methyl ends of the PCDA molecules (the center of the image in Figure 1a) is somewhat more prominent in the positive bias image, but this is not a consistent effect and is tentatively attributed to the tip state here. The polymer nanowires, not the unpolymerized molecules, thus exhibit a unique effect even when the bias voltage magnitude is the same, as is the case in Figure 5. Numerous images acquired with many different tips at other bias voltage magnitudes, multivolt or otherwise, have confirmed these results.

Figure 6 shows a set of images on MoS_2, again acquired using the same multivolt imaging method. Unlike the case with HOPG, the nanowires here are the same apparent height as, and thus are indistinguishable from, the surrounding PCDA layer at positive sample bias voltages. The PCDA layer is clearly visible at both polarities. Surprisingly, at positive voltages, a structure resembling the PCDA layer in terms of height and spatial periodicity is visible where the PDA nanowires should be. It should be stressed that the nanowires are still on the surface during the positive bias scan, yet none of the PDA electronic states are probed by the tunneling electrons. Again, this has also been confirmed on many different samples with images acquired both using multivolt imaging and by numerous sequential scans of the same area at both positive and negative bias voltages.

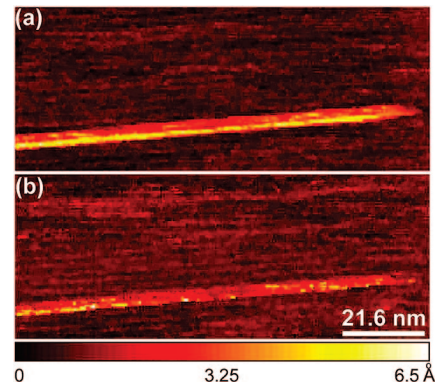

Figure 5. STM images of PDA nanowires on HOPG acquired simultaneously at (a) −1.0 V and (b) +1.0 V, both with the same color scale [0.0 to 6.5 Å]. Each line was acquired at both voltages during the scan. The nanowires are clearly visible in the +1 V scan, as is the PCDA monolayer. The nanowires are less bright at +1 V relative to the background, indicating a change in electronic properties with respect to voltage bias polarity. Imaging conditions for both (a) and (b): 10 pA, 108 × 51 nm^2.

The bright points in the positive bias image are due to surface defects; a close comparison with the negative bias image reveals the defects at the same locations, though they are far smaller and less prominent at negative sample bias voltages. In fact, the defects hidden beneath nanowires in the negative image are visible in the positive image, indicating that the STM is tunneling directly through the nanowires in the positive voltage case. Positive bias voltages up to +1.5 V did not reveal any nanowires on MoS_2.

Voltage-dependent imaging provides a simple method for extracting spectroscopic structure from the specific surface features of interest.[36] For example, changing the bias voltage while scanning semiconductors has been known to produce different images, even without changing the polarity of the bias voltage.[38] Numerous images of PDA nanowires on both HOPG and MoS_2 were thus acquired at many different bias voltages, and the average nanowire heights were measured. In a number of cases, the gap resistance was kept constant in order to prevent the tip from piercing the film. Because of the different tunneling conditions for various samples and experiments, a range of height values was found at different bias voltages.

The general trend across a range of bias voltages is evident in Figure 7, which plots the measured nanowire heights at different bias voltages. The heights were measured on numerous nanowires from different samples at each bias voltage using the averaging method described briefly above and in detail in the Methods section below. Each data point is an average of the average height values at each voltage. In total, this plot represents the heights measured on approximately 230 different PDA nanowires from 22 different samples. The error bars indicate the standard error in the mean nanowire height value and are a result of at least three factors: the difference in image clarity between negative and positive bias images, the different tips used, and the various current setpoints used for different samples at each bias voltage that affect the tip position. Different setpoints were sometimes used, for example, to maintain the same approximate tip height at different bias voltages. In all cases, only straight nanowires surrounded by a highly ordered PCDA monolayer were considered, in which case these were probably "blue phase" PDA nanowires.[39]

Because the tunneling current is related to the density of states (DOS) at a particular bias voltage, the height of the tip is related to the integrated DOS of both the tip and substrate up to that energy. The height−voltage measurements here, particularly in the case of single samples where the same gap height is maintained at each voltage, provide substantial (if indirect) spectroscopic information about the system. The plotted height values are related to the electronic structure at the interface and also contain information about gap narrowing in the PDA nanowires as well as the influence of substrate effects such as doping, charging, and electron screening. The data in Figure 7 can thus also provide a qualitative understanding of the Fermi level position within the PDA. In addition, the height values might help to explain the gap narrowing observed *via* d*I*/d*V* spectra of PDA nanowires on HOPG.[19,20]

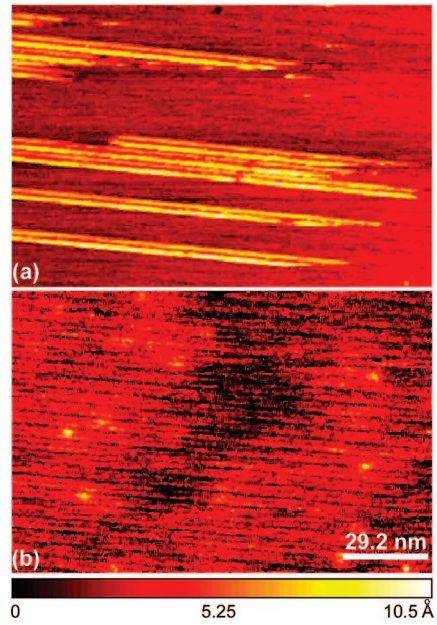

Figure 6. STM images of PDA nanowires on MoS_2 acquired simultaneously line-by-line at (a) −1.0 V and (b) +1.0 V. Although the PCDA monolayer is easily discernible in the positive bias image, none of the nanowires appear. The bright points in (b) are surface defects, which are smaller but evident in (a), and in fact in (b) some of the surface defects hidden beneath the nanowires in (a) are imaged. Imaging conditions for both (a) and (b): 8 pA, 146 × 98 nm^2.

The height−voltage measurements described here are also different from *z*−*V* spectroscopy measurements reported elsewhere.[40–43] In a *z*−*V* experiment, the feedback loop is kept closed while the bias voltage is swept. This method has the effect of moving the tip into the polymer at lower bias voltages with the purpose of determining the so-called "single particle gap" in the system. A *z*−*V* measurement does not provide any information on whether a structure's height actually changes with respect to bias voltage because the tip height, rather than the nanostructure height, is measured. Particularly at lower bias voltages, the current in our experiments was often changed to keep the tip at approximately the same height above the nanowire, thus allowing for determination of the nanowire height without direct contact with the tip. This is not the case in *z*−*V* experiments. On PDA nanowires, piercing the polymer causes irreparable damage, such as inducing desorption,[11,13,14] making accurate determination of the single-particle gap impossible.

Four features in the height data in Figure 7 stand out: a decrease in nanowire height as the bias voltage magnitude-dependent approaches 0 V, evidence of im-

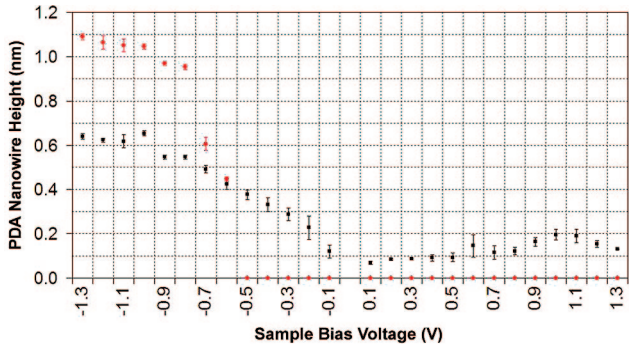

Figure 7. The height of PDA nanowires on HOPG (black) and MoS_2 (red) analyzed at sample bias voltages from −1.3 to +1.3 V, indicating bias dependence in the nanowire height due to electronic effects. The error bars indicate the standard error in the mean height value at each voltage. Nanowire heights were determined by averaging the height cross section of each wire, as was done in Figure 4. The increased error at positive bias voltages is due to less stable imaging conditions in this regime. On HOPG, the height decreases as the voltage magnitude approaches 0 V, and the height is much greater at negative bias voltages than at equivalent positive bias voltages. These two trends indicate the decreasing density of states due to the finite band gap and the substrate−polymer charge transfer interaction effect, respectively. On MoS_2, the height decreases more rapidly, and no nanowires were visible at voltages above −0.6 V. The asymmetry in the height−voltage data on HOPG and the extreme asymmetry in the data on MoS_2 reflect the substrate-dependent electronic effects when imaging the PDA nanowires. Comparing the two indicates a definite role of the substrate in determining PDA nanowire height.

aging within the band gap of PDA, an asymmetrical height−voltage profile on HOPG and MoS_2, and the lack of nanowires at substrate bias voltages greater than −0.6 V on MoS_2. Bulk PDA has a reported gap between the highest occupied molecular orbital (HOMO) and lowest unoccupied molecular orbital (LUMO) of 2.34[44] to 2.5 eV,[45] while PDA nanowires on HOPG have a reported gap as small as 0.5 eV.[20] In Figure 7, nanowires are clearly visible on HOPG at bias voltages within the band gap. The asymmetry on both HOPG and MoS_2 is due to the change in carriers and the band alignment in the system, particularly the location of the Fermi level (E_F) in the nanowire. For HOPG, the measured heights at positive bias voltages are far less than those at negative bias voltages; for MoS_2, the height values drop rapidly between −0.8 and −0.6 V, with no data points for any voltages beyond that at negative or positive voltages. The nature of PDA nanowires in STM images is thus peculiar and requires a discussion of a large number of possible sources that contribute to both trends evident in Figure 7, such as substrate-induced doping, screening by the substrate, polymer charging, polymer−electrode coupling issues, surface dipole and work function-related issues, band banding and rectification on MoS_2, and the electronic structure of PDA. Thus far, in the relevant literature, substrate-dependent factors have been largely ignored, possibly because reports of STM analysis of PDA nanowires have only focused on HOPG substrates. An assessment of the contribution of these factors to the data points in Figure 7 follows.

The decrease in measured heights as the bias voltage magnitude approaches 0 V is likely due to the energy gap present in the PDA nanowires.[20,44–46] As the sample bias voltage magnitude is reduced, the level being probed approaches the edge of the HOMO−LUMO gap. This results in limited tunneling probability, given that the density of states (DOS) in the nanowire is lower near the band gap. The decrease in heights occurs even if the gap resistance is kept constant across the different bias voltages (*i.e.*, the current is reduced along with the bias voltage).

Doping effects are probably involved in the asymmetry data. Because of the HOMO−LUMO gap in the nanowires, PDA is a poor conductor and should be more difficult to image using STM unless there is some doping or charge transfer effect due to the substrate. For example, the graphite substrate arguably supplies holes to the nanowire.[9,20] Figure 7 supports the idea of p-type doping given that hole transfer (at negative bias voltages) is far more efficient than electron transfer (at positive bias voltages). The result is a shift in E_F closer to the HOMO level. If the PDA nanowires were unaffected by the substrate, then the nanowires would appear with the same height on both substrates. Substrate-induced doping might thus also partially explain why the nanowires are taller on MoS_2 substrates. The initial assumption given the increase of nanowire height at negative substrate bias voltages is that the MoS_2 substrate p-type dopes the nanowire more than HOPG. This is consistent with the observation that naturally occurring MoS_2 (as was used here) is typically p-type doped. The difference in doping may be due to the surface sulfur atoms on MoS_2, which cleaves between adjacent sulfur planes. Figure 8 shows possible energy band diagrams for PDA nanowires on HOPG and MoS_2, respectively, using the work function and gap values noted earlier as well as a work function of 4.8 eV for the Pt:Rh tip.[47] PDA is positioned based on an ionization potential of 5.1 eV.[48] The influence of the PDA HOMO−LUMO gap on tunneling is evident through each set of images. Doping moves E_F closer to the HOMO level, and there is thus a larger gap before conduction can take place at positive sample biases (assuming LUMO and HOMO band conduction at positive and negative biases, respectively). Because MoS_2 possibly dopes the PDA backbone more than HOPG, E_F is positioned closer to the HOMO level on MoS_2. The smaller the difference between E_F and the HOMO level, the more asymmetric the resulting $I-V$ curve and height−voltage plot.

This asymmetry can also be described in terms of charge transfer efficiency between the nanowire and the substrate. If the nanowires interact more strongly with MoS_2 than HOPG at negative bias voltages (that is, if hole injection is highly efficient), then that would cause the nanowire to appear taller on MoS_2 in negative voltage images. Similarly, if the nanowires exhibit

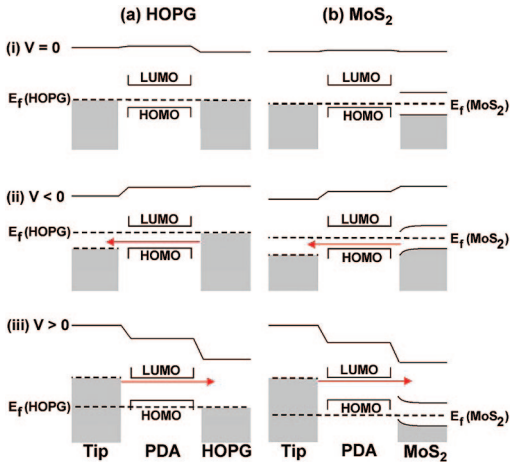

Figure 8. Illustrative energy band diagrams for PDA nanowires on (a) HOPG and (b) MoS_2 at (i) 0 V, (ii) negative bias voltage, and (iii) increasing positive bias voltage. The schematics in (ii) show the onset of conduction when E_F in HOPG or the valence band maximum in MoS_2 are equal to the PDA HOMO level. In (iii), conduction begins when the E_F level in the tip is equal to the PDA LUMO level for both substrates. Work function values and the PDA HOMO−LUMO levels are shown approximately to scale based on the values in the text. Arrows indicate possible mechanisms for conduction.

weak electron transfer, then the nanowires would appear shorter on HOPG; if the electron transfer is extraordinarily weak, the nanowire may not appear at all.

Screening effects may additionally explain why the HOMO−LUMO gap on these materials is much smaller than the measured bulk value. For ordered monolayers of poly(3-dodecylthiophene) (P3DDT) on HOPG, screening by the substrate was offered as the cause for narrowing the gap from 1.48 to 0.93 eV.[49,50] Screening occurs due to the transient charge on the polymer during the tunneling process. In the PDA system, the tunneling is in two steps: from the tip to the PDA nanowire and from the PDA nanowire to the substrate (or *vice versa*, depending on the voltage polarity). During tunneling, PDA can have a net charge due to the finite tunneling time required (either an extra electron in the LUMO level or a hole in the HOMO level), which causes an increased HOMO−LUMO gap in the polymer due to the shift in the respective orbitals. This self-energy effect[50] in the nanowire is then screened by the substrate or tip, thus effectively reducing the PDA HOMO−LUMO gap. The degree to which screening occurs is related to the substrate. Metals, such as HOPG, probably screen more strongly than semiconductors such as MoS_2,[51] thus E_F may be farther from the HOMO on HOPG than on MoS_2. Screening is also important for keeping the molecular orbital levels fixed under an applied bias.[52] As MoS_2 probably screens the PDA internal charge less than HOPG, the HOMO and LUMO levels may not be constant over the bias range.

Differing degrees of coupling asymmetry[50,53,54] in the tip−PDA−substrate system can also contribute to the difference in heights on HOPG *versus* MoS_2. Such coupling concerns are related to work function issues that affect the PDA height. The work function of a material comprises both its bulk component and its surface dipole. It is well-established that the tails of the electron states in the substrate due to its surface dipole can allow for STM imaging of otherwise insulating molecules such as xenon,[55] which is in part one of the reasons that PDA can be imaged at biases less than the energy of the HOMO−LUMO gap. An organic adsorbate, even if physisorbed as is the case here, has an effect on the surface dipole.[56] The tails of the electron states in the metal that extend out into the polymer are "pushed back" due to repulsion from the adsorbate electrons.[57] The end result is a reduction in the substrate work function, which accordingly shifts the PDA energy levels downward relative to E_F and increases the hole injection barrier at the interface. A decrease in the hole injection barrier would result in lower asymmetry in the height−voltage curve in Figure 7. Clearly, this surface dipole effect is related to the substrate material. This increases the difference in asymmetry between the data on HOPG and on MoS_2. As noted above, the work function of the two substrates differs by approximately 0.25 eV. These values are based on bulk measurements, however, and do not account for changes in the work function due to the adsorbate and associated surface dipole effects. Even if the surface dipole-induced reduction is minimal, the mere difference in work functions between HOPG and MoS_2 would still cause a difference in the hole injection barrier between the two substrates and would thus help explain the difference in height values. The hole injection efficiency on MoS_2 would be higher than on HOPG because E_F would necessarily be closer to the HOMO level in PDA.[58] This is shown in Figure 8 by the different vacuum-level alignments due to the work function values of HOPG and MoS_2.

Lastly, the transparency of the nanowires at positive substrate bias voltages on MoS_2 must be addressed. One possibility is that the band alignment of MoS_2 with that of PDA prevents the overlap of LUMO states with that of the conduction band in MoS_2. However, the states of MoS_2 must overlap to at least some degree with those of the unpolymerized PCDA molecules given that the monolayer is evident at all bias conditions. That a PCDA-like structure is evident at positive voltages where PDA nanowires should be is due to the interaction between the polymer and the substrate, so even if the system is tunneling through the nanowires the local variation in barrier height is similar to that of the PCDA layer.[36]

The rectifying effect of MoS_2 may also limit tunneling at positive voltages, as was noted for copper phthalocyanine.[59] Being a semiconductor, MoS_2 will exhibit an accumulation or depletion effect at the MoS_2−PDA interface depending on the applied bias, similar to that exhibited by silicon at the poly(3-hexylthiophene)−silicon interface.[51] Such an effect results in band bend-

ing at the interface, as depicted in Figure 8. The resulting rectification effect limits tunneling, particularly at low bias regimes, and is probably responsible for the lack of PDA nanowire images beyond −0.6 V in Figure 7. Depending on how strong the band bending is, this could also determine what means of conduction are possible in the system. As mentioned above, highly inefficient electron transfer efficiency may also prevent nanowire imaging at positive bias voltages.

The various factors described here can help explain both the observed nanowire height asymmetry in Figure 7 as well as the difference in height on HOPG and MoS_2. A shift in the PDA nanowire Fermi level, which contributes to $I-V$ and height$-V$ asymmetry, can be caused by substrate doping, screening, or surface dipole effects. The reduction in the HOMO−LUMO gap from the bulk PDA value to that of PDA nanowires on HOPG is probably due to charge screening effects, as was found for P3DDT on HOPG. PDA nanowires on HOPG can be imaged within the HOMO−LUMO gap due to the tail of the electronic states from the substrate overlapping the Fermi level even within the gap. Each of these issues is substrate-dependent and thus may explain the difference in height values between PDA nanowires on HOPG *versus* those on MoS_2. Additionally, rectification by the MoS_2 substrate may help explain why nanowires do not appear at positive sample biases.

CONCLUSIONS

We have utilized scanning tunneling microscopy to investigate the substrate-dependent behavior in polydiacetylene nanowires. Voltage-dependent averaged height cross sections of the PDA nanowires show a change in electronic behavior due to the substrate material. The substrate used thus plays a critical role in PDA nanowire devices such as interconnects in molecular circuitry. The results presented here demonstrate the first atomic-scale insight into this phenomenon on polydiacetylene. Further analysis with complementary surface techniques, particularly various scanning probe spectroscopy methods, as well as on other layered substrates will hopefully provide additional insights beyond the data presented here.

METHODS

Polydiacetylene nanowires were formed by polymerizing an ordered monolayer film of 10,12-pentacosadiynoic acid (PCDA) molecules.[60] The PCDA molecules were deposited in two ways. In the first process, PCDA was deposited on the substrates using a Langmuir−Schaefer (LS) deposition technique[61] as reported previously.[14,62] Specifically, 10 μL of a 0.75 mg/mL solution of PCDA dissolved in chloroform was deposited on a surface of ultrapure (~18 MΩ) water. The PCDA monolayer films were transferred onto freshly cleaved HOPG and MoS_2 substrates[63] using a commercial trough apparatus.[64] This method, while difficult, results in a single layer of molecules.

In addition to LS deposition, ordered PCDA films were also formed by heating the substrate in air to approximately 480 K and then drop-casting 2 μL of a 0.75 mg/mL (2 mM) solution of PCDA dissolved in chloroform onto the heated substrate. This method allows for much faster, more reliable sample preparation as compared to that on LS films. Nanowires were formed by irradiating the surface with 254 nm UV light[65] in a UV-filtered environment. The UV lamp was held from 3 to 8 cm above each sample, and the irradiation times varied from 1 to 10 min. This created nanowires of varying lengths at random locations on the surface. STM images of surfaces prepared by both methods revealed no difference in terms of structure, ordering, or nanowire height. It should be noted that deposition was attempted on several other substrates, such as gold, iodine-on-gold, tantalum disulfide, and aluminum, but STM scans of these samples did not reveal any ordered films.

Images were acquired with cut platinum:rhodium (80:20) tips using a home-built STM[66] operated by commercial RHK electronics in ambient conditions. All images were acquired in the constant current mode of operation, and the voltage bias in all images was applied to the sample. Images were processed in MATLAB to correct for piezo drift and were then converted to TIFF images using Adobe Photoshop Elements. The images in Figure 2 were processed using WSxM.[67]

The nanowire heights were measured using a custom MATLAB script. It should be noted that determining nanowire heights on a periodic background such as the PCDA monolayer can, if not done carefully, result in misleading data. This is because measuring nanowire heights not only requires selecting a reasonable upper bound but also requires a consistent baseline with limited manual input in order for the heights across different nanowires to be compared with any confidence. The baseline here is the average height of the surrounding PCDA monolayer. The method to select the baseline must be consistent for each measurement; as noted in Figure 1, the height profile across each stripe has a range of 0.2 nm. Specifically, a box was drawn to include the nanowire of interest as well as the surrounding PCDA monolayer. The height profiles along each line perpendicular to the nanowire within the selected region were averaged together, producing a mean height profile. The nanowire height was then determined by subtracting the mean height of the PCDA monolayer on each side of selected nanowire from the peak nanowire height. Mean height measurements on numerous nanowires were taken at each of the bias voltages shown in Figure 7. The mean nanowire height measurements at each bias were then averaged to produce each point on the plot. The error bars are the standard error in the mean nanowire height. This was used only for samples where an ordered monolayer was clearly visible and where the nanowires were linear; in other words, care was taken to not include any possible "red-phase" nanowires[39] in the height measurements. As noted in the main text, the plot includes data on approximately 230 different PDA nanowires from 22 different samples. The images were median filtered prior to measurement to eliminate the influence of noise spikes on the height measurement.

Acknowledgment. We thank J. H. Hafner for Langmuir−Blodgett equipment. R.G. is supported by a National Science Foundation Graduate Research Fellowship. This work is funded by the Rochester MURI on Nanoscale Subsurface Spectroscopy and Tomography (F49620-031-0379) administered by the Air Force Office of Scientific Research, and the National Science Foundation (ECS0601303).

REFERENCES AND NOTES

1. Bürgi, L.; Richards, T. J.; Friend, R. H.; Sirringhaus, H. Close Look at Charge Carrier Injection in Polymer Field-Effect Transistors. *J. Appl. Phys.* **2003**, *94*, 6129–6137.
2. Gundlach, D. J.; Zhou, L.; Nichols, J. A.; Jackson, T. N.; Necliudov, P. V.; Shur, M. S. An Experimental Study of Contact Effects in Organic Thin Film Transistors. *J. Appl. Phys.* **2006**, *100*, 024509-1–024509-13.

3. Yaliraki, S. N.; Ratner, M. A. Molecule-Interface Coupling Effects on Electronic Transport in Molecular Wires. *J. Chem. Phys.* **1998**, *109*, 5036–5043.
4. Engelkes, V. B.; Beebe, J. M.; Frisbie, C. D. Length-Dependent Transport in Molecular Junctions Based on SAMs of Alkanethiols and Alkanedithiols: Effect of Metal Work Function and Applied Bias on Tunneling Efficiency and Contact Resistance. *J. Am. Chem. Soc.* **2004**, *126*, 14287–14296.
5. Takami, K.; Kuwahara, Y.; Ishii, T.; Akai-Kasaya, M.; Saito, A.; Aono, M. Significant Increase in Conductivity of Polydiacetylene Thin Film Induced by Iodine Doping. *Surf. Sci.* **2005**, *591*, L273–L279.
6. Day, D. R.; Lando, J. B. Conduction in Polydiacetylene Bilayers. *J. Appl. Polym. Sci.* **1981**, *26*, 1605–1612.
7. Sakamoto, M.; Wasserman, B.; Dresselhaus, M. S.; Wnek, G. E.; Elman, B. S.; Sandman, D. J. Enhanced Electrical Conductivity of Polydiacetylene Crystals by Chemical Doping and Ion Implantation. *J. Appl. Phys.* **1986**, *60*, 2788–2796.
8. Okawa, Y.; Aono, M. Nanoscale Control of Chain Polymerization. *Nature* **2001**, *409*, 683–684.
9. Okawa, Y.; Aono, M. Linear Chain Polymerization Initiated by a Scanning Tunneling Microscope Tip at Designated Positions. *J. Chem. Phys.* **2001**, *115*, 2317–2322.
10. Miura, A.; De Feyter, S.; Abdel-Mottaleb, M. M. S.; Gesauirère, P.; Grim, P. C. M.; Moessner, G.; Sieffert, M.; Klapper, M.; Müllen, K.; De Schryver, F. C. Light- and STM-Tip-Induced Formation of One-Dimensional and Two-Dimensional Organic Nanostructures. *Langmuir* **2003**, *19*, 6474–6482.
11. Takajo, D.; Okawa, Y.; Hasegawa, T.; Aono, M. Chain Polymerization of Diacetylene Compound Multilayer Films on the Topmost Surface Initiated by a Scanning Tunneling Microscope Tip. *Langmuir* **2007**, *23*, 5247–5250.
12. Nishio, S.; I.-i., D.; Matsuda, H.; Yoshidome, M.; Uji-i, H.; Fukumura, H. Formation of Molecular Wires by Nanospace Polymerization of a Diacetylene Derivative Induced with a Scanning Tunneling Microscope at a Solid−Liquid Interface. *Jpn. J. Appl. Phys.* **2005**, *44*, 5417–5420.
13. Sullivan, S. P.; Schnieders, A.; Mbugua, S. K.; Beebe, T. P., Jr. Controlled Polymerization of Substituted Diacetylene Self-Organized Monolayers Confined in Molecule Corrals. *Langmuir* **2005**, *21*, 1322–1327.
14. Giridharagopal, R.; Kelly, K. F. STM-Induced Desorption of Polydiacetylene Nanowires and Reordering *via* Molecular Cascades. *J. Phys. Chem. C* **2007**, *111*, 6161–6166.
15. Manaka, T.; Kohn, H.; Ohshima, Y.; Lim, E.; Iwamoto, M. Direct Observation of Trapped Carriers in Polydiacetylene Films by Optical Second Harmonic Generation. *Appl. Phys. Lett.* **2007**, *90*, 171119-1–171119-3.
16. Zou, G.; Lim, E.; Tamura, R.; Kajimoto, N.; Manaka, T.; Iwamoto, M. Surface Morphology and Electrical Transport Properties of Polydiacetylene-Based Organic Field-Effect Transistors. *Jpn. J. Appl. Phys* **2006**, *45*, 6436–6441.
17. Scott, J. C.; Samuel, J. D. J.; Hou, J. H.; Rettner, C. T.; Miller, R. D. Monolayer Transistor Using a Highly Ordered Conjugated Polymer as the Channel. *Nano Lett.* **2006**, *6*, 2916–2919.
18. Wang, Y.; Yang, K.; Wang, X.; Nagarajan, R.; Samuelson, L. A.; Kumar, J. *In Situ* Polymerization of Amphiphilic Diacetylene for Hole Transport in Solid State Dye-Sensitized Solar Cells. *Org. Electron.* **2006**, *7*, 546–550.
19. Akai-Kasaya, M.; Yamamoto, Y.; Saito, A.; Aono, M.; Kuwahara, Y. Polaron Injection into a One-Dimensional Polydiacetylene Nanowire. *Jpn. J. Appl. Phys.* **2006**, *45*, 2049–2052.
20. Akai-Kasaya, M.; Shimizu, K.; Saito, A.; Aono, M.; Kuwahara, Y. Electronic Structure of a Polydiacetylene Nanowire Fabricated on Highly Ordered Pyrolytic Graphite. *Phys. Rev. Lett.* **2003**, *91*, 255501-1–255501-4.
21. Yoffe, A. D. Electronic Properties of Some Chain and Layer Compounds. *Chem. Soc. Rev.* **1976**, *5*, 51–78.
22. Weimer, M.; Kramar, J.; Bai, C.; Baldeschwieler, J. D. Tunneling Microscopy of 2H-MoS_2: A Compound Semiconductor Surface. *Phys. Rev. B* **1988**, *37*, 4292–4295.
23. Kelly, K. F.; Halas, N. J. Determination of α and β Site Defects on Graphite Using C_{60}-Adsorbed STM Tips. *Surf. Sci.* **1998**, *416*, L1085–L1089.
24. Schlaf, R.; Lang, O.; Petternkoger, C.; Jaegermann, W. Band Lineup of Layered Semiconductor Heterointerfaces Prepared by van der Waals Epitaxy: Charge Transfer Correction Term for the Electron Affinity Rule. *J. Appl. Phys.* **1999**, *85*, 2732–2753.
25. McMenamin, J. C.; Spicer, W. E. Photoemission Studies of Layered Transition-Metal Dichalcogenides: MoS_2. *Phys. Rev. B* **1977**, *16*, 5474–5487.
26. Hansen, W. N.; Hansen, G. J. Standard Reference Surfaces for Work Function Measurements in Air. *Surf. Sci.* **2001**, *281*, 172–184.
27. Maeda, F.; Takahashi, T.; Ohsawa, H.; Suzuki, S. Unoccupied-Electronic-Band Structure of Graphite Studied by Angle-Resolved Secondary-Electron Emission and Inverse Photoemission. *Phys. Rev. B* **1988**, *37*, 4482–4488.
28. Chen, C. J. *Introduction to Scanning Tunneling Microscopy*; Oxford University Press: New York, 1993.
29. Hibino, M.; Sumi, A.; Hatta, I. Atomic Images of Saturated and Unsaturated Fatty Acids at Liquid/Graphite Interface and Difference of Tunneling Currents between Them Observed by Scanning Tunneling Microscopy. *Jpn. J. Appl. Phys.* **1995**, *34*, 610–614.
30. Sasaki, D. Y.; Carpick, R. W.; Burns, A. R. High Molecular Orientation in Mono- and Trilayer Polydiacetylene Films Imaged by Atomic Force Microscopy. *J. Colloid Interface Sci.* **2000**, *229*, 490–496.
31. Giancarlo, L. C.; Fang, H.; Rubin, S. M.; Bront, A. A.; Flynn, G. W. Influence of the Substrate on Order and Image Contrast for Physisorbed, Self-Assembled Molecular Monolayers: STM Studies of Functionalized Hydrocarbons on Graphite and MoS_2. *J. Phys. Chem. B* **1998**, *102*, 10255–10263.
32. Hara, M.; Iwakabe, Y.; Tochigi, K.; Sasabe, H.; Garito, A. F.; Yamada, A. Anchoring Structure of Smectic Liquid-Crystal Layers on MoS_2 Observed by Scanning Tunneling Microscopy. *Nature* **1990**, *344*, 228–230.
33. Grévin, B.; Rannou, P.; Payerne, R.; Pron, A.; Travers, J.-P. Multi-Scale Scanning Tunneling Microscopy Imaging of Self-Organized Regioregular Poly(3-hexylthiophene) Films. *J. Chem. Phys.* **2003**, *118*, 7097–7102.
34. Cyr, D. M.; Venkataraman, B.; Flynn, G. W. STM Investigations of Organic Molecules Physisorbed at the Liquid−Solid Interface. *Chem. Mater.* **1996**, *8*, 1600–1615.
35. Okawa, Y.; Takajo, D.; Tsukamoto, S.; Hasegawa, T.; Aono, M. Atomic Force Microscopy and Theoretical Investigation of the Lifted-Up Conformation of Polydiacetylene on a Graphite Substrate. *Soft Matter* **2008**, *4*, 1041–1047.
36. Wiesendanger, R. *Scanning Probe Microscopy and Spectroscopy: Methods and Applications*. Cambridge University Press: Cambridge, UK, 1994.
37. Lackinger, M.; Müller, T.; Gopakumar, T. G.; Müller, F.; Hietschold, M.; Flynn, G. W. Tunneling Voltage Polarity Dependent Submolecular Contrast of Naphthalocyanine on Graphite. A STM Study of Close-Packed Monolayers under Ultrahigh-Vacuum Conditions. *J. Phys. Chem. B* **2004**, *108*, 2279–2284.
38. Becker, R.; Wolkow, R. Semiconductor Surfaces: Silicon. In *Scanning Tunneling Microscopy*; Stroscio, J. A., Kaiser, W. J., Eds.; Academic Press, Inc.: San Diego, CA, 1993; pp 149−224.
39. Saito, A.; Urai, Y.; Itoh, K. Infrared and Resonance Raman Spectroscopic Study on the Photopolymerization Process of the Langmuir−Blodgett Films of a Diacetylene Monocarboxylic Acid, 10,12-Pentacosadiynoic Acid. *Langmuir* **1996**, *12*, 3938–3944.
40. Alvarado, S. F.; Barth, S.; Bässler, H.; Scherf, U.; van der Horst, J.-W.; Bobbert, P. A.; Michels, M. A. J. Spatially Resolved STM Spectroscopy of Charge Injection at the Ladder-Type Poly(*para*-phenylene)/Au(111) Interface. *Adv. Funct. Mater.* **2002**, *12*, 117–122.

41. Alvarado, S. F.; Seidler, P. F.; Lidzey, D. G.; Bradley, D. D. C. Direct Determination of the Exciton Binding Energy of Conjugated Polymers Using a Scanning Tunneling Microscope. *Phys. Rev. Lett.* **1998**, *81*, 1082–1085.
42. Kemerink, M.; Alvarado, S. F.; Müller, P.; Koenraad, P. M.; Salemink, H. W. M.; Wolter, J. H.; Janssen, R. A. J. Scanning Tunneling Spectroscopy on Organic Semiconductors: Experiment and Model. *Phys. Rev. B* **2004**, *70*, 045202-1–045202-13.
43. Kemerink, M.; Offermans, P.; van Duren, J. K. J.; Koenraad, P. M.; Janssen, R. A. J.; Salemink, H. W. M.; Wolter, J. H. Real-Space Measurement of the Potential Distribution Inside Organic Semiconductors. *Phys. Rev. Lett.* **2002**, *88*, 096803-1–096803-4.
44. Sebastian, L.; Weiser, G. One-Dimensional Wide Energy Bands in a Polydiacetylene Revealed by Electroreflectance. *Phys. Rev. Lett.* **1981**, *46*, 1156–1159.
45. Sariciftci, N. S.; Kraabel, B.; Lee, C. H.; Pakbaz, K.; Heeger, A. J. Absence of Photoinduced Electron Transfer from the Excitonic Electron-Hole Bound State in Polydiacetylene Conjugated Polymers. *Phys. Rev. B* **1994**, *50*, 12044–12051.
46. Brédas, J. L.; Change, R. R.; Silbey, R.; Nicholas, G.; Durand, P. A Nonempirical Effective Hamiltonian Technique for Polymers: Application to Polyacetylene and Polydiacetylene. *J. Chem. Phys.* **1981**, *75*, 255–267.
47. Ishii, R.; Matsumura, K.; Sakai, A.; Sakata, T. Work Function of Binary Alloys. *Appl. Surf. Sci.* **2001**, *169−170*, 658–661.
48. Seki, K.; Morisada, I.; Tanaka, H.; Edamatsu, K.; Yoshiki, M.; Takata, Y.; Yokoyama, T.; Ohta, T.; Asada, S.; Inokuchi, H.; Nakahara, H.; Fukuda, K. Photopolymerization of Long-Chain Diacetylene Monocarboxylic Acid in Langmuir−Blodgett Films Studied by UV Photoelectron Spectroscopy and X-ray Absorption Near-Edge Structure. *Thin Solid Films* **1989**, *179*, 15–20.
49. Scifo, L.; Dubois, M.; Brun, M.; Rannou, P.; Latil, S.; Rubio, A.; Grévin, B. Probing the Electronic Properties of Self-Organized Poly(3-dodecylthiophene) Monolayers by Two-Dimensional Scanning Tunneling Spectroscopy Imaging at the Single Chain Scale. *Nano Lett.* **2006**, *6*, 1711–1718.
50. Dubois, M.; Latil, S.; Scifo, L.; Grévin, B. Scanning Tunneling Spectroscopy Simulations of Poly(3-dodecylthiophene) Chains Adsorbed on Highly Oriented Pyrolytic Graphite. *J. Chem. Phys.* **2006**, *125*, 034708-1–034708-9.
51. Terada, Y.; Miki, K.; Fujimori, M.; Heike, S. S. Y.; Hashizume, T. Electronic Structure of a Polymer Nanowire on H-Terminated Si(100). *J. Appl. Phys.* **2005**, *97*, 124302-1–124302-6.
52. Terada, Y.; Choi, B.-K.; Heike, S.; Fujimori, M.; Hashizume, T. Placing Conducting Polymers onto a H-Terminated Si(100) Surface *via* a Pulse Valve. *Nano Lett.* **2003**, *3*, 527–531.
53. Tian, W.; Datta, S.; Hong, S.; Reifenberger, R.; Henderson, J. I.; Kubiak, C. P. Conductance Spectra of Molecular Wires. *J. Chem. Phys.* **1998**, *109*, 2874–2882.
54. Zahid, F.; Ghosh, A. W.; Paulsson, M.; Polizzi, E.; Datta, S. Charging-Induced Asymmetry in Molecular Conductors. *Phys. Rev. B* **2004**, *70*, 245317-1–245317-5.
55. Eigler, D. M.; Weiss, P. S.; Schweizer, E. K.; Lang, N. D. Imaging Xe with a Low-Temperature Scanning Tunneling Microscope. *Phys. Rev. Lett.* **1991**, *66*, 1189–1192.
56. Crispin, X.; Geskin, V.; Crispin, A.; Cornil, J.; Lazzaroni, R.; Salaneck, W. R.; Brédas, J. L. Characterization of the Interface Dipole at Organic/Metal Interfaces. *J. Am. Chem. Soc.* **2002**, *124*, 8131–8141.
57. Koch, N.; Kahn, A.; Ghijsen, J.; Pireaux, J.-J.; Schwartz, J.; Johnson, R. L.; Elschner, A. Conjugated Organic Molecules on Metal *versus* Polymer Electrodes: Demonstration of a Key Energy Level Alignment Mechanism. *Appl. Phys. Lett.* **2003**, *82*, 70–72.
58. Forsythe, E. W.; Gao, Y. Interfaces in Organic Light-Emitting Devices. In *Handbook of Surfaces and Interfaces of Materials*; Nalwa, H. S., Ed.; Academic Press: San Diego, CA, 2001; Vol. 1, pp 286−328.
59. Ludwig, C.; Strohmaier, R.; Peterson, J.; Gompf, B.; Eisenmenger, W. Epitaxy and Scanning Tunneling Microscopy Image Contrast of Copper−Phthalocyanine on Graphite and MoS_2. *J. Vac. Sci. Technol., B* **1994**, *12*, 1963–1966.
60. Purchased from Sigma-Aldrich.
61. Langmuir, I.; Schaefer, V. J. The Effect of Dissolved Salts on Insoluble Monolayers. *J. Am. Chem. Soc.* **1937**, *59*, 2400–2414.
62. Kuroda, R.; Kishi, E.; Yamano, A.; Hatanaka, K.; Matsuda, H.; Eguchi, K.; Nakagiri, T. Scanning Tunneling Microscope Images of Fatty Acid Langmuir−Blodgett Bilayers. *J. Vac. Sci. Technol., B* **1991**, *9*, 1180–1183.
63. Both purchased from SPI, www.2spi.com.
64. Kibron, Inc., http://www.kibron.com.
65. Model Spectroline 11SC-1, Sigma-Aldrich.
66. Kelly, K. F.; Sarkar, D.; Prato, S.; Resh, J. S.; Hale, G. D.; Halas, N. J. Direct Observation of Fullerene-Adsorbed Tips by Scanning Tunneling Microscopy. *J. Vac. Sci. Technol., B* **1996**, *14*, 593–596.
67. Horcas, I.; Fernandez, R.; Gomez-Rodriguez, J. M.; Colchero, J.; Gomez-Herrero, J.; Baro, A. M. WSXM: A Software for Scanning Probe Microscopy and a Tool for Nanotechnology. *Rev. Sci. Instrum.* **2007**, *78*, 013705-1–013705-8.